EPJ Web of Conferences **38**, 14001 (2012)
DOI: 10.1051/epjconf/20123814001

Inner crust of neutron stars with finite range interactions

Nguyen Van Giai[1,a], Elias Khan[1,b], and Zhongyu Ma[2,c]

[1] Institut de Physique Nucléaire, Université Paris-Sud, 91405 Orsay, France
[2] CIAE, P.O. Box 275-18, Beijing 102413, P.R. China

Abstract. The microscopic structure of the inner crust of neutron stars is generally studied in the framework of local energy density functionals (EDF). Here, we discuss other possible frameworks, either based on non-relativistic EDF which are fully non-local, or covariant EDF of the relativistic mean field (RMF) type. These other approaches must be more widely used in the context of neutron stars in order to gain confidence in predicting general trends.

1 Introduction

Neutron stars are important astrophysical objects whose study shed light on numerous and diverse properties of physical systems, ranging from the evolution of supernovae to the behavior of baryonic matter at various densities. The inner crust of the neutron star is a particularly interesting region of this compact stellar object, where many physical processes are taking place. For instance, it is central for determining the cooling time of the neutron star, and it is probably the region where the glitch phenomenon originates as a result of the sudden unpinning of vortices. It is thus necessary to understand the nuclear structure of the inner crust, a system made mostly of neutrons and a smaller number of protons and electrons in electrical equilibrium. Electrons are delocalized, while protons and neutrons are gathered around the sites of a Wigner-Seitz lattice with the excess neutrons forming a uniform medium filling the space.

The first microscopic study of the inner crust of neutron stars in a nuclear physics context goes back to the seminal work of Negele and Vautherin[1]. Two main ideas were introduced: each density zone is represented by a Wigner-Seitz cell whose radius, the number of neutrons and protons - N and Z - inside the cell and the energy per particle E/A are determined respectively by the β-equilibrium conditions, and by minimizing the Hartree-Fock (HF) energy of the cell. With the choice of effective nucleon-nucleon interaction made in Ref. [1] Negele and Vautherin found that, in the region of inner crust with densities ranging from $10^{-3}\rho_0$ to $0.5\rho_0$ (ρ_0 being the nuclear matter saturation density) one could define about 10 zones of increasing density and in each zone, the optimal values of N and Z, as well as the corresponding cell radius R, were determined. These zones with the corresponding (N,Z) numbers are presented in Table 1. It is customary to characterize the content of a cell by the name of the nucleus having that Z number and the atomic mass A=N+Z.

Based on this early determination of the composition of the inner crust, a large number of studies of the neutron star properties have been performed within various mean field models: Hartree-Fock (HF), Hartree-Fock-BCS (HF-BCS), Hartree-Fock-Bogoliubov (HFB). It is not our purpose to give here a detailed list of references, and we simply mention one of the recent HFB investigations[2] where more references can be found. These investigations were based on Skyrme-type effective interactions, with the exception of the work reported in [3] where the EDF was built from the Fayans functional supplemented with Brueckner-HF nuclear matter inputs, and where a redetermination of the (N,Z) numbers was carried out. In some cases substantial differences with the Negele-Vautherin values were found, pointing to the necessity in future studies to recalculate Table 1 for each particular EDF which is used.

Here, we want to examine theoretical frameworks that are alternative to the commonly used zero-range, Skyrme-type EDF. Such attempts are not very numerous, and we shall discuss two of them. The first one is still a non-relativistic, self-consistent mean field approach but the effective interactions are of finite range. The second one is the covariant, self-consistent relativistic mean field (RMF) approach which is quite successful in describing finite nuclei.

2 Inner crust with non-relativistic finite range interactions

The HF method with finite range interactions is well known [4–7] and we shall not enter into many details here. Writing the single-particle wave functions as

$$\varphi_i(\boldsymbol{r},\sigma,q) = \frac{u_\alpha(r)}{r}\mathcal{Y}_{ljm}(\hat{r},\sigma)\chi_q(\tau), \qquad (1)$$

the radial wave functions $u_\alpha(r)$ and single-particle energies ϵ_α are solutions of the self-consistent set of HF equations

[a] e-mail: nguyen@ipno.in2p3.fr
[b] e-mail: khan@ipno.in2p3.fr
[c] e-mail: mazy12@ciae.ac.cn

Table 1. The Wigner-Seitz cells considered in this work. ρ, N, Z and R_{WS} are the baryonic densities, the numbers of neutrons and protons, and the WS cell radii, respectively. ρ_0=0.16 fm^{-3} is the nuclear matter saturation density. All values are taken from Ref. [1].

N_{zone}	ρ/ρ_0	N	Z	$R_{WS}[fm]$
10	0.143×10^{-2}	140	40	53.6
9	0.250×10^{-2}	160	40	49.2
8	0.375×10^{-2}	210	40	46.3
7	0.549×10^{-2}	280	40	44.3
6	0.994×10^{-2}	460	40	42.2
5	0.233×10^{-1}	900	50	39.3
4	0.361×10^{-1}	1050	50	35.7
3	0.557×10^{-1}	1300	50	33.1
2	1.275×10^{-1}	1750	50	27.6
1	2.968×10^{-1}	1460	40	19.6
0	4.931×10^{-1}	950	32	14.4

$$
\begin{aligned}
&-\frac{\hbar^2}{2m}[u_i^{''}(r_1) - \frac{l_i(l_i+1)}{r_1^2}u_i(r_1)] \\
&+ U_i^D(r_1)u_i(r_1) - \int U_i^E(r_1,r_2)u_i(r_2)r_2^2 dr_2 \\
&+ [j_i(j_i+1) - l_i(l_i+1) - \frac{3}{4}]W^{LS}(r_1)u_i(r_1) = \epsilon_i u_i(r_1),
\end{aligned}
\tag{2}
$$

where U_i^D, U_i^E and W^{LS} are respectively the Hartree (local), Fock (non-local) and spin-orbit self-consistent potentials. Their analytical expressions in terms of single-particle wave functions and two-body interactions can be found, e.g., in [7] where the numerical methods for solving these HF equations are also discussed.

The HF calculations are done with finite-range interactions (the D1S [5] and M3Y-P4 [6] forces) imposing Dirichlet-Neumann boundary conditions at the edge of the cell as introduced in Ref. [1]. These boundary conditions for the single-particle wave functions are taken as follows: (i) the even parity wave functions vanish at the edge $r = R_{WS}$ of the box; (ii) the first derivative of the odd-parity wave functions vanish at $r = R_{WS}$. The purpose of these chosen boundary conditions is to obtain an approximately constant density at large distance from the center of the cell, thus simulating a lattice of nucleus-like systems embedded in a uniform neutron gas. The influence of the choice of boundary conditions is discussed in Ref. [3].

It should be noted that the more physical Bloch boundary conditions could be used at the cost of more complex calculations as presented in Refs. [8,9]. The validity in neutron star crust of the Wigner-Seitz approximation that we use here has been discussed in [8].

The effects of pairing correlations are known to be substantial in the inner crust, and it is necessary to include them to obtain a more realistic picture. Here, we adopt the simplified HF-BCS description, although a full Hartree-Fock-Bogoliubov (HFB) treatment would be ultimately required. The results presented here have been obtained by using in the particle-particle channel either a zero-range, density-dependent pairing force, or finite-range pairing forces as explained in Ref. [7].

We can now examine the predictions of the different models based on zero-range or finite-range forces in the particle-hole channel. Let us first compare the Hartree-Fock results obtained either with Skyrme-type, or finite-range type interactions. The first observation is that, in the outer part of the inner crust, the central densities are smaller with finite range interactions (D1S, M3Y-P4) than with zero range forces (SLy4). This is illustrated in figure 1. A closer examination of the shell occupations shows that this difference comes from the different filling of some neutron $s_{1/2}$ orbitals in the different models. This trend fades away as one goes towards more inner regions of the crust, as shown in figure 2.

In the innermost zones of Table 1 one can see clearly from figure 2 that the picture of spherically symmetric distributions of neutrons and protons around the sites of a lattice and immersed in a neutron gas of constant density start to fail. Indeed, the density of the outer neutron gas does not seem quite constant in zone 1, and in zone 0 the picture breaks down. This is the sign that the spherical symmetry assumption for the clusters no longer hold there, and deformation effects must be taken into account for this part of the inner crust where the so-called pasta phase appears.

The HF-BCS calculations of Ref. [7] performed with the D1S interaction also shed some light on the effect of pairing correlations on the density profiles inside the Wigner-Seitz cells. It is found that, moving from the outer region towards the center the pairing effects are affecting very little the density profiles in the regions 5 and 4 of Table 1. However, in the regions 3, 2 and 1 there are sizable changes in the density distributions due to pairing effects. This is due to the depletion in the occupancy of the $8s_{1/2}$ neutron level which produces a 10% reduction of the central neutron density. This type of study shows that, among other motivations, it would be desirable to have a better knowledge of the in-medium nuclear interaction in the pairing channel since various properties of the inner crust depend on that interaction.

A further remark concerns the use of the Negele-Vautherin crust composition for this type of study. In Ref. [7] the energies per nucleon in the Wigner-Seitz cells calculated with the interaction D1S were compared to those of a β-stable uniform gas of neutrons, protons and electrons. The gain in energy is significant by considering a Coulomb lattice of proton and neutron clusters in a neutron gas. This gain with respect to the gas can be up to 4 MeV, which is more in some cases than with the Wigner-Seitz calculations based on Table 1. Only for the zone 1 of Table 1, the E/A value of the gas is 15 keV lower than that calculated with D1S. This points to the necessity to perform a full optimisation of the crust composition for different interaction models.

3 Inner crust with covariant EDF

The vast majority of microscopic studies of the neutron star inner crust are based on non-relativistic energy density functionals or effective nucleon-nucleon interactions. Because of the success of the relativistic mean field (RMF) model in dealing with the properties of atomic nuclei it is natural to explore with this covariant method the structure of neutron stars[10]. Let us start with the Lagrangian of the

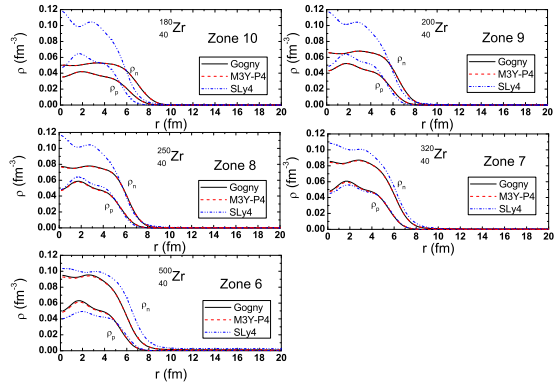

Fig. 1. The HF proton and neutron density profiles in the five outermost zones of Table 1. The interactions used correspond to D1S[5], M3Y-P4[6] and SLy4[11].

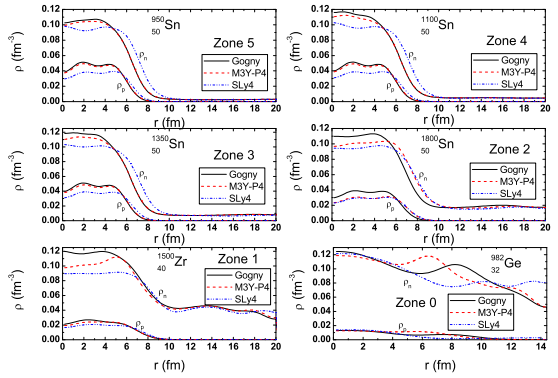

Fig. 2. Same as figure 1, but for the 6 innermost zones of Table 1.

RMF model with density-dependent couplings

$$\mathcal{L} = \bar{\psi}\left(i\gamma\cdot\partial - m\right)\psi + \frac{1}{2}(\partial\sigma)^2 - \frac{1}{2}m_\sigma^2\sigma^2 - \frac{1}{4}\Omega_{\mu\nu}\Omega^{\mu\nu} + \frac{1}{2}m_\omega^2\omega^2 - \frac{1}{4}\mathrm{R}_{\mu\nu}\mathrm{R}^{\mu\nu} + \frac{1}{2}m_\rho^2\rho^2 - \frac{1}{4}\mathrm{F}_{\mu\nu}\mathrm{F}^{\mu\nu} - g_\sigma(\rho_v)\bar{\psi}\sigma\psi - g_\omega(\rho_v)\bar{\psi}\gamma^\mu\omega_\mu\psi - g_\rho(\rho_v)\bar{\psi}\gamma^\mu\rho_\mu\cdot\tau\psi - e\bar{\psi}\gamma\cdot A\frac{(1-\tau_3)}{2}\psi\,, \tag{3}$$

where the nucleon-meson couplings depend on the baryonic density ρ_v. The parameter set DDME1[12] will be used in the rest of this study.

The nucleon spinors can be decomposed into their radial and spin-angular components

$$\psi_i(\mathbf{r}) = \begin{pmatrix} i\frac{G_{ik}(r)}{r}\mathcal{Y}^l_{jm}(\hat{r}) \\ \\ \frac{F_{ik}(r)}{r}(\sigma\cdot\hat{r})\mathcal{Y}^l_{jm}(\hat{r}) \end{pmatrix}\chi_i, \tag{4}$$

where $\mathcal{Y}^l_{jm}(\hat{r})$ is a spin 1/2 spinor coupled with a spherical harmonic Y_l to a total angular momentum (jm). The radial parts of the nucleon spinors satisfy the Dirac equation

$$\begin{aligned}\epsilon_i G_{ik}(r) &= (-\frac{d}{dr} + \frac{\kappa}{r})F_{ik}(r) \\ &\quad + [M + S(r) + V_0(r) + \Sigma_0^R(r)]G_{ik}(r)\,, \\ \epsilon_i F_{ik}(r) &= (\frac{d}{dr} + \frac{\kappa}{r})G_{ik}(r) \\ &\quad - [M + S(r) - V_0(r) - \Sigma_0^R(r)]F_{ik}(r)\,. \end{aligned} \tag{5}$$

$S(r)$, $V_0(r)$ and $\Sigma_0^R(r)$ are the scalar, vector and rearrangement potentials, respectively[12]. The pairing properties are calculated in the BCS approximation as in the previous section, using the finite range Gogny force.

The main technical difference with the previous non-relativistic model is the choice of boundary conditions at the edge of the Wigner-Seitz cell. In order to insure a flat density tail outside the central cluster, one chooses to impose in the non-relativistic case that the wave function (resp. its derivative) be zero at the cell boundary R_c if l is even (resp. odd). This ensures a flat density tail while maintaining the orthogonality of the wave functions. In RMF one must generalize this prescription, and one possible choice preserving the orthogonality is

$$\begin{cases} G_{nk}(R_c) = 0, & l \text{ even}, \\ F_{nk}(R_c) = 0, & l \text{ odd}. \end{cases} \tag{6}$$

We show now some examples of applications where the parameters of the RMF Lagrangian are those of Ref. [12] whereas the pairing force is taken as the Gogny interaction[4]. In figure 3 the density distributions with and without pairing correlations for $\rho = 0.12\rho_0$ and $Z = 50$, $N = 1750$(zone 2 of Table 1) are compared. One can notice that the core and the tail of the neutron density distribution with pairing are flatter than those without pairing.

In figure 4 are shown the neutron pairing gaps for the different quasiparticle states in the cell ^{1800}Sn corresponding to the zone 2 of Table 1. There is an overall linear energy dependence of the gaps, similarly to the behavior of the pairing gap in neutron matter. One can observe that the maximum of Δ_n is about 4 MeV and the corresponding single-particle energy is around -10 MeV, which corresponds to the depth of the neutron gas potential. The presence of the core nucleus in the Wigner-Seitz cell leads to a reduction of the gap by about 0.5 MeV. This behavior of the neutron pairing gap is quite similar to that obtained in a non-relativistic mean field approach with the Gogny pairing force by Pizzochero et al. [13]. It is also found that the pairing gaps in this W-S cell are larger than those obtained in finite nuclei[14].

4 Conclusion

In this work we have studied the properties of W-S cells in the inner crust of neutron stars using two different types of self-consistent mean field approaches, firstly non-relativistic mean fields generated by finite-range self-consistent nuclear interactions, and secondly covariant mean fields built from relativistic Lagrangians. Both types of approaches are very successful in describing finite nuclei and therefore, it is reasonable to apply them to the study of neutron stars. Their predictions of the properties of the inner crust

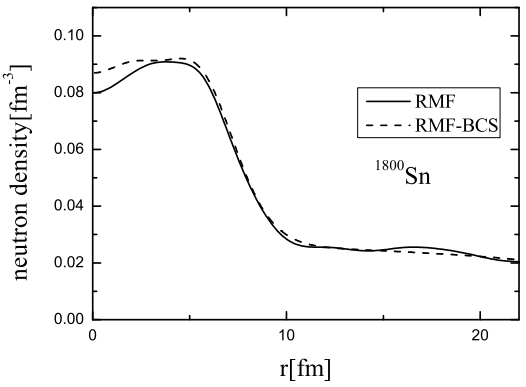

Fig. 3. Neutron density distributions in the zone 2 of Table 1, in RMF and RMF-BCS.

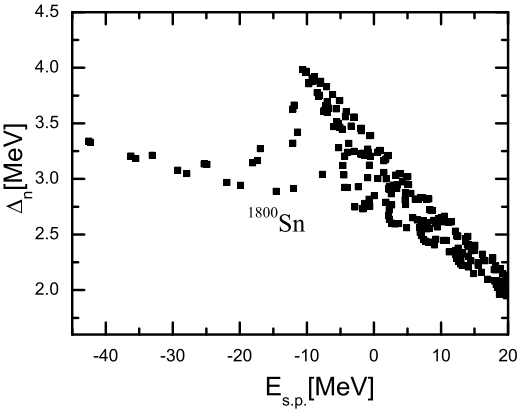

Fig. 4. The neutron pairing gaps $\Delta_n$in the zone 2 of Table 1, calculated with Gogny interaction as a function of neutron single-particle energies.

are quite comparable, and not very different from those of Skyrme-type energy density functionals. This should not be too surprising since these different approaches generally agree on the bulk properies of finite nuclei. Finally, an important step needs to be taken towards determining the optimal neutron/proton crust composition for each energy density functional, covariant or not, if one looks for reliable predictions with new energy functionals or effective interactions.

Acknowledgments

We wish to thank Hoang Sy Than and Cao Jiguang for their important contribution to the results presented here.

References

1. J.W. Negele, D. Vautherin, Nucl. Phys. A **207**, 298 (1973)
2. F. Grill, J. Margueron, N. Sandulescu, Phys. Rev. C **84**, 065801 (2011)
3. M. Baldo, E.E. Saperstein, S.V. Tolokonnikov, Nucl. Phys. A **775**, 235 (2006)
4. J. Dechargé, D. Gogny, Phys. Rev. C **21**, 1568 (1980)
5. J.-F. Berger, M. Girod, D. Gogny, Comput. Phys. Comm. **63**, 365 (1991)
6. H. Nakada, Phys. Rev. C **78**, 054301 (2008)
7. Hoang Sy Than, E. Khan, N. Van Giai, J. Phys. G: Nucl. Part. Phys. **38**, 025201 (2011)
8. N. Chamel, S. Naimi, E. Khan, J. Margueron, Phys. Rev. C **75**, 055806 (2007)
9. N. Chamel, J. Margueron, E. Khan, Phys. Rev. C **79**, 012801 (R) (2009)
10. Jiguang Cao, Zhongyu Ma, N. Van Giai, Int. J. Mod. Phys. E **17**, 1765 (2008)
11. E. Chabanat, P. Bonche, P. Haensel, J. Meyer, R. Schaeffer, Nucl. Phys. A **635**, 231 (1998)
12. T. Niksic, D. Vretenar, P. Finelli, P. Ring, Phys. Rev. C **66**, 024306 (2002)
13. P.M.Pizzochero, F.Barranco, R.A.Broglia, Astrophys. J. **569**, 381 (2002)
14. M.Serra, P.Ring, Phys. Rev. C **65**, 064324 (2002)